Journal of Neuroinflammation

RESEARCH

Open Access

Accumulated BCAAs and BCKAs contribute to the HFD-induced deterioration of Alzheimer's disease via a dysfunctional TREM2-related reduction in microglial β-amyloid clearance

Yang Yang[1], Guanjin Shi[1], Yanyan Ge[1], Shanshan Huang[1], Ningning Cui[1], Le Tan[1], Rui Liu[2*] and Xuefeng Yang[1*]

Abstract

A high-fat diet (HFD) induces obesity and insulin resistance, which may exacerbate amyloid-β peptide (Aβ) pathology during Alzheimer's disease (AD) progression. Branched-chain amino acids (BCAAs) accumulate in obese or insulin-resistant patients and animal models. However, roles of accumulated BCAAs and their metabolites, branched-chain keto acids (BCKAs), in the HFD-induced deterioration of AD and the underlying mechanisms remains largely unclear. In this study, APPswe/PSEN1dE9 (APP/PS1) transgenic mice were fed a HFD for 6 months, and the BCAAs content of the HFD was adjusted to 200% or 50% to determine the effects of BCAAs. The HFD-fed APP/PS1 mice accumulated BCAAs and BCKAs in the serum and cortex, which was accompanied by more severe cognitive deficits and AD-related pathology. The additional or restricted intake of BCAAs aggravated or reversed these phenomena. Importantly, BCAAs and BCKAs repressed microglial phagocytosis of Aβ in vivo and in BV2 cells, which might be relevant for triggering receptor expressed on myeloid cells 2 (TREM2) dysfunction and autophagy deficiency. We found that BCAAs and BCKAs could bind to TREM2 in silico, in pure protein solutions and in the cellular environment. These molecules competed with Aβ for binding to TREM2 so that the response of TREM2 to Aβ was impaired. Moreover, BCAAs and BCKAs decreased TREM2 recycling in an mTOR-independent manner, which might also lead to TREM2 dysfunction. Our findings suggest that accumulated BCAAs and BCKAs contribute to the HFD-induced acceleration of AD progression through hypofunctional TREM2-mediated disturbances in Aβ clearance in microglia. Lowering BCAAs and BCKAs levels may become a potential dietary intervention for AD.

Keywords Alzheimer's disease, HFD, Insulin resistance, BCAAs, BCKAs, Amyloid-β, Microglia, TREM2

Introduction

Alzheimer's disease (AD) is one of the most prominent neurodegenerative diseases and is accompanied by a progressive decline in memory and cognitive functions [1]. Many factors may contribute to the pathophysiology of AD, including environmental, genetic, and metabolic disorders. Increasing evidence indicates a relationship between type 2 diabetes mellitus (T2DM) and AD [2, 3]. Amyloid-β peptide (Aβ) plaques in the brain constitute the hallmark pathology of AD, the pathogenic significance of which has been documented in several studies

*Correspondence:
Rui Liu
LiuR@jhun.edu.cn
Xuefeng Yang
xxyxf@hust.edu.cn
[1] Department of Nutrition and Food Hygiene, Hubei Key Laboratory of Food Nutrition and Safety, MOE Key Laboratory of Environment and Health, School of Public Health, Tongji Medical College, Huazhong University of Science and Technology, Wuhan, Hubei 430030, People's Republic of China
[2] Department of Public Health and Preventive Medicine, School of Medicine, Jianghan University, Wuhan, Hubei 430010, People's Republic of China

[4–6]. Insulin resistance and obesity, which are T2DM-related factors, are associated with cognitive impairment in AD patients [2, 7]. A high-fat diet (HFD) causes complex metabolic disturbances, including insulin resistance and obesity, which have been reported to aggravate Aβ pathology in an AD mouse model [8]. These findings reveal that HFD-induced metabolic disorders play causal roles in AD progression. Recent studies have suggested that insulin resistance and obesity are related to an imbalance in branched-chain amino acids (BCAAs) [9, 10]. Branched-chain keto acids (BCKAs) dehydrogenase activity in peripheral tissues is inhibited by diet induced-insulin resistance or obesity such that BCAAs accumulate in the circulation [11–13]. The brain is an important BCAAs reactor in which BCAAs serve as a nitrogen source for the synthesis of the neurotransmitter glutamate [14]. However, excessive BCAAs in the brain lead to neurotoxicity and neurological dysfunction, which may promote the development of neurodegenerative diseases [15]. Moreover, elevated BCAAs levels are also found in AD patients and AD mouse models [16, 17], indicating that BCAAs metabolic disorders are potentially linked to AD progression. Nevertheless, whether an impaired BCAAs balance is involved in the HFD-induced deterioration of AD remains largely unclear.

Several studies have shown that HFD feeding interrupts microglial clearance of Aβ and the function of triggering receptor expressed on myeloid cells 2 (TREM2) in research models [18–20]. Microglia are the primary immune cells of the central nervous system and act as important scavengers of Aβ during AD progression [21]. Loss of the response to Aβ in senescence-associated microglia may accelerate the development of early-stage AD [22]. TREM2 is a cell surface receptor that drives microglial phagocytosis of Aβ [23]. Evidence has shown that patients with TREM2 mutations have a substantial increase in the risk of developing AD [24]. Repressed microglial responses to Aβ and increased amyloid burdens have also been reported in AD mice deficient in TREM2 or expressing the hypofunctional $TREM2^{R47H}$ human variant [25, 26], suggesting that TREM2 is critical for Aβ clearance by microglia. Although the effects of BCAAs on microglial immune properties have been discovered in vitro [27, 28], how BCAAs influence Aβ phagocytosis in microglia needs to be explored. Some ligands, such as lipoproteins, phospholipids and Aβ, are able to bind to TREM2 [29], wherein Aβ contacts TREM2 to induce microglial phagocytosis of Aβ in a spleen tyrosine kinase (SYK)-dependent manner [25, 30]. However, whether BCAAs and their metabolites BCKAs are ligands for TREM2 is unknown. Furthermore, autophagy, a catabolic process that sequesters the cytoplasm, plays a neuroprotective role in AD [31]. Microglial autophagy is involved in the maintenance of TREM2 function, which enables microglia to degrade extracellular Aβ, and a microglial autophagy deficiency gives rise to senescence-associated microglia with decreased TREM2 expression [22, 32]. In addition, other evidence has shown that noncanonical autophagy (LC3-associated endocytosis), rather than canonical autophagy, supports microglial TREM2 recycling, in which TREM2 is endocytosed and returns to the plasma membrane for the efficient clearance of Aβ [33]. BCAAs can suppress autophagic activity through mTOR activation, but whether BCAAs and BCKAs affect TREM2 via autophagy has not been elucidated. Here, we hypothesize that BCAAs and BCKAs impact the microglial phagocytosis of Aβ by binding to TREM2 and interfering with TREM2 function and autophagy.

Therefore, this study aimed to determine the effects of excessive BCAAs and BCKAs on the HFD-induced deterioration of AD and the underlying molecular mechanisms involved. We used APPswe/PSEN1dE9 (APP/PS1) transgenic mice to establish an HFD-feeding AD model. The BCAAs contents of the HFD group were adjusted to investigate the role of BCAAs in AD progression. Results showed that BCAAs and BCKAs significantly accumulate in the serum and cortex of HFD-fed mice. Higher BCAAs and BCKAs levels were correlated with worse cognitive function and AD-related pathology. In addition, we showed that BCAAs and BCKAs restrained microglial phagocytosis of Aβ through alterations in TREM2 function. BCAAs/BCKAs formed bonds with TREM2 and reduced TREM2 expression and recycling through canonical and noncanonical autophagy, respectively, thereby disrupting the response of TREM2 to Aβ. This study provides evidence for a better understanding of the role of diet-induced metabolic disorders in promoting AD progression.

Materials and methods

Animal model and experimental protocol

Three-month-old male APP/PS1 transgenic mice were obtained from Beijing HFK Bioscience (Beijing, China). The mice were maintained with ad libitum access to food and water at 25 ± 1 °C, 50%–60% relative humidity and a 12 h light/dark cycle. After adaptation for 1 week, the mice were randomly divided into chow, HFD, HFD + BCAAs and HFD-BCAAs groups and fed a chow diet (10% of energy from fat with protein as free amino acids, A08051501, Research Diets Inc., New Brunswick, NJ, USA), a HFD (45% of energy from fat with protein as free amino acids, A06071304, Research Diets Inc.), or a HFD plus 100% BCAAs or minus 50% BCAAs (based on A06071304, Beijing HFK Bioscience, Beijing, China) for 6 months. The details of the diets are listed in Table S1.

Each group contained 11–12 mice, and the group sizes were designed based on previous studies [8, 13] and obeyed the principle of 3Rs (reduction, replacement and refinement). All procedures were approved by the Ethics Committee of Tongji Medical College of Huazhong University of Science and Technology (IACUC number: 2946), and complied with animal biomedical research principles formulated by the China Animal Care Committee and the Council of the International Medical Organization.

Oral glucose tolerance test (OGTT)

Food was withdrawn from the cages for 12 h before the experiments. The mice were intragastrically administered glucose (1 g/kg body weight), then blood samples were collected from the tail vein at the times indicated in the figures, and the blood glucose levels were measured with an Accu-Chek Performa glucometer.

Morris water maze

The Morris water maze experiments were performed to test spatial learning and memory functions, as previously described [25]. A circular pool (120 cm in diameter) with nontoxic opacified water (23 ± 2 °C) was equally divided into four logical quadrants, and a platform (12 cm in diameter) was placed 1 cm beneath the water in quadrant IV (target quadrant). Spatial cues were distributed around the pool. Before the experiment, the mice were allowed to adapt to the environment of the testing room. During the training period, the mice were allowed 60 s to find the platform and 15 s to stay on the platform. If the mice failed to find the platform within 60 s, they were guided to it and allowed to remain there for 15 s. The training session lasted for 5 consecutive days, with four trials per day. On the sixth day, the hidden platform was removed, and a 60 s probe test for memory retention was performed. The swimming activity of each mouse was automatically recorded by the digital tracking software SuperMaze (Shanghai Xinruan Information Technology, Shanghai, China).

Metabolic measurements

Blood samples were collected, incubated at room temperature for 1 h, and then centrifuged at 2000 × g for 10 min to obtain the serum supernatant. Serum concentrations of glucose, total triglyceride (TG), total cholesterol (TC), high-density lipoprotein cholesterol (HDL-C) and low-density lipoprotein cholesterol (LDL-C) were determined under fasting conditions using the corresponding assay kits (Nanjing Jiancheng Bioengineering Institute, Nanjing, Jiangsu, China). Fasting serum insulin levels were measured using a mouse insulin ELISA kit (Elabscience Biotechnology, Wuhan, Hubei, China).

Amino acids and BCKAs detection by LC–MS/MS

The levels of 19 amino acids and 3 BCKAs in the serum and cortex were quantified via LC–MS/MS according to previous methods [34, 35]. Analytical separation was performed on a Waters ACQUITY UPLC H-Class PLUS system (Waters, Milford, MA, USA) equipped with a ZORBAX RRHD Eclipse Plus C18 column (95 Å, 3.0 × 150 mm, 1.8 μm; Agilent Technologies, Wilmington, DE, USA). Mass spectra were recorded using a Xevo TQ-XS MS/MS (Waters) with an electrospray ionization (ESI) source. The scan type was set as switching polarity (positive/negative) multiple reaction monitoring (MRM) mode. The standards were all purchased from MedChemExpress (Shanghai, China).

For the serum analysis, 40 μL of serum was mixed with 160 μL of a methanol solution (containing 0.1% formic acid) containing an internal standard consisting of norvaline (5 μg/mL) and salicylic acid (0.45 μg/μL). The mixture was centrifuged at 12,000 × *g* for 10 min at 4 °C to precipitate the protein, and the supernatant was collected for analysis.

For the analysis of the cortex, the cortex was harvested from mouse, snap frozen in liquid nitrogen and stored at − 80 °C. The tissue was homogenized in a 1:10 (w/v) volume of methanol/deionized water (1:1, v/v, 0.1% formic acid, prechilled at − 20 °C) and then centrifuged at 12,000 × *g* for 10 min at 4 °C. A total of 100 μL of the supernatant was transferred to a centrifuge tube containing 300 μL of 0.1% formic acid in methanol containing internal standards. After centrifugation at 12,000 × *g* for 10 min at 4 °C, the supernatant was obtained for analysis.

ELISA analysis for APP and Aβ

The cortex of mouse was homogenized with TBS followed by centrifugation at 12,000 × *g* for 20 min at 4 °C. The supernatant was collected as soluble fraction, and the pellet was solubilized in 70% formic acid as insoluble fraction. Amyloid precursor protein (APP) from soluble fraction and total $A\beta_{1-40}$ and $A\beta_{1-42}$ (including soluble and insoluble fraction) were measured using corresponding ELISA kits (Elabscience Biotechnology) according to the manufacturer's instructions. Protein concentration in each sample was measured by BCA assays (Nanjing Jiancheng Bioengineering Institute).

Immunohistochemistry

Mouse brains were fixed with 4% paraformaldehyde in PBS for 24 h, dehydrated and embedded in paraffin until use. Immunohistochemical staining was performed as previously described [36]. The primary antibodies used included rabbit polyclonal anti-BCAT1 (ab232706, Abcam, Shanghai, China), rabbit polyclonal anti-BCAT2

(ab95976, Abcam), mouse monoclonal anti-6E10 (SIG-39320, Covance, Princeton, NJ, USA), and rabbit polyclonal anti-IBA1 (ab178846, Abcam) antibodies. Appropriate secondary antibodies were used for immunohistochemical and immunofluorescence staining.

For immunohistochemical and immunofluorescence staining, images were captured using an Axio Observer 7 (ZEISS, Oberkochen, BW, Germany) and processed with ZEN software. Quantification of the images was performed using ImageJ software. The proper threshold was used for quantification. Cortex and hippocampus regions from the brain section were analyzed, respectively. Mean intensity of BCAT1 and BCAT2 signal and Aβ plaque-positive area were measured, and IBA1-positive cell number were counted. Aβ plaque-positive area and IBA1-positive cell number were normalized to region area.

For Aβ plaque-associated microglia analysis, images were acquired using a confocal microscope (Nikon, Tokyo, Japan) and processed with NIS-elements software. IBA1-positive cell number within a 20-μm range from Aβ plaques was counted, and normalized to Aβ plaques area according to previous studies with some modification [18, 36].

Quantitative real-time polymerase chain reaction

Total RNA was extracted from the mouse cortex, purified and concentrated using an RNA Easy Fast Tissue/Cell Kit (TIANGEN Biotechnology, Beijing, China). Total RNA was reverse transcribed into cDNA using a FastKing RT kit (TIANGEN Biotechnology). Real-time PCR was performed using PowerUp SYBR Green mix (Thermo Fisher Scientific, Waltham, MA, USA) and an Applied Biosystems 7900HT thermocycler. Threshold cycle values were normalized to those of GAPDH. The specific primers used in this study are listed in Table S2.

BV2 cell culture and treatments

Mouse microglial BV2 cells were purchased from Servicebio Technology (Wuhan, China). BV2 cells were cultured in complete Dulbecco's modified Eagle's medium (DMEM) containing penicillin and streptomycin in a 37 °C incubator with 5% CO_2. Aggregation of $A\beta_{1-42}$ (MedChemExpress) was conducted as previously described [36]. Briefly, $A\beta_{1-42}$ was aggregated for 24 h at 37 °C. Unless indicated otherwise, BV2 cells were treated with vehicle, BCAAs (5 mM, leucine: valine: isoleucine = 1:1:1) or BCKAs (5 mM, KICA:KMVA:KIVA = 1:1:1) in the presence of Aβ (1 μM) with or without 40 μM sphingosine-1-phosphate (S1P; MedChemExpress) for 4 h. In addition, BV2 cells were treated with vehicle, BCAAs or BCKAs in the presence of Aβ with or without the agents rapamycin (50 nM), chloroquine (40 μM) or 4-octyl itaconate (40 μM) (MedChemExpress) for 12 h.

Western blotting

Cortical samples and BV2 cells (2×10^5 cells per well) were homogenized in RIPA lysis buffer containing protease and phosphatase inhibitor tablets (Beyotime Biotechnology, Shanghai, China), lysed on ice for 30 min, and then centrifuged at 12,000 × g for 10 min at 4 °C. The supernatants were added to SDS–PAGE sample loading buffer (Beyotime Biotechnology), denatured at 100 °C for 10 min and then analysed by immunoblotting. The primary antibodies used were as follows: rabbit polyclonal anti-BCAT2 (ab95976, Abcam), rabbit polyclonal anti-BCKDK (ab111716, Abcam), rabbit polyclonal anti-phospho-BCKDH (ab200577, Abcam), rabbit monoclonal anti-BCKDH (90198, Cell Signaling Technology, Danvers, MA, USA), rabbit monoclonal anti-synaptophysin (5461, Cell Signaling Technology), rabbit polyclonal anti-PSD95 (A7889, ABclonal Technology, Wuhan, Hubei, China), rabbit polyclonal anti-BACE1 (A5266, ABclonal Technology), rabbit polyclonal anti-IBA1 (ab178846, Abcam), rabbit monoclonal anti-TREM2 (ab305103, Abcam), rabbit monoclonal anti-phospho-Zap-70/SYK (2717, Cell Signaling Technology), rabbit polyclonal anti-SYK (A2123, ABclonal Technology), rabbit polyclonal anti-phospho-p70 S6 kinase (AP0564, ABclonal Technology), rabbit monoclonal anti-p70 S6 kinase (A4898, ABclonal Technology), rabbit monoclonal anti-LC3A/B (12741, Cell Signaling Technology), rabbit monoclonal anti-SQSTM1/P62 (A19700, ABclonal Technology), rabbit monoclonal anti-RUBIUCON (8465, Cell Signaling Technology) and rabbit polyclonal anti-GAPDH (ab9485, Abcam) antibodies. Appropriate secondary antibodies were used for Western blotting. ImageJ software was used to perform the greyscale analysis.

Aβ phagocytosis and degradation assays

Microglial phagocytosis and degradation of aggregated $A\beta_{1-42}$ were analysed using previously described methods [33, 36]. Before the experiments, HiLyte™ Fluor 488-Aβ1–42 (AS-60479, AnaSpec, Fremont, CA, USA) was aggregated for 24 h at 37 °C. BV2 cells were plated at a density of 2×10^4 cells per well in BeyoGold™ white 96-well cell culture plates with clear bottoms (Beyotime Biotechnology) and incubated overnight. For the phagocytosis assays, BCAAs (5 mM) or BCKAs (5 mM) with fluorescein labelled-Aβ (1 μM) were simultaneously added to the BV2 cells, and the extracellular Aβ was removed before each measurement. For degradation assays, BV2 cells were treated with fluorescein labelled-Aβ for 2 h and washed twice with DMEM, followed by the addition of BCAAs or BCKAs. The

fluorescence was recorded at a 503-nm excitation wavelength and 528-nm emission wavelength at the indicated times in the figures.

Furthermore, microglial Aβ phagocytosis was verified via fluorescence microscopy. Briefly, 1×10^5 cells were plated in 24-well plates. After treatment with the BCAAs or BCKAs with fluorescein labelled-Aβ in the presence or absence of S1P (40 μM) for 4 h, an anti-IBA1 antibody and DyLight 594-labelled secondary antibody were used to label the cell shape, and 4′,6-diamidino-2-phenylindole (DAPI) was used to stain the nuclei. BV2 cells were treated with BCAAs or BCKAs with unlabelled Aβ in the presence or absence of rapamycin (50 nM), chloroquine (40 μM) or 4-octyl itaconate (40 μM) for 12 h, after which the culture medium was replaced, and fluorescein-labelled Aβ was added. Finally, the cells were subjected to fluorescence staining 2 h later and photographed with an Axio Observer 7 (ZEISS). The amount of intracellular Aβ in the images was quantified using ImageJ software.

Molecular docking

The molecular docking simulation was performed with Autodock Vina (National Biomedical Computation Resource). The crystal structure of the TREM2 extracellular domain (PDB ID: 6YYE) was downloaded from the RCSB Protein Data Bank (http://www.rcsb.org/pdb). The protein molecules were prepared via correction, removal of ligands and water, and the addition of hydrogen. The binding sites were set as described in previous reports [37, 38]. The 3D structures of the ligands were generated from PubChem (National Library of Medicine) and prepared in AutoDock Vina. After docking, the results were visualized using Discovery Studio Visualizer (Dassault Systèmes, Vélizy-Villacoublay, France).

Biolayer interferometry (BLI) assay

The binding affinities of the BCAAs and BCKAs for TREM2 were measured using the ForteBio Octet 96e system (SARTORIUS AG, Göttingen, NI, Germany). The recombinant human TREM2 protein was obtained from R&D Systems (Minneapolis, MN, USA). After biotin labelling, the TREM2 protein (0.5 mg/mL) was immobilized on a specific streptavidin sensor. The sensor was washed and incubated with bovine serum albumin to block redundant sites. The concentrations of the BCAAs and BCKAs ranged from 15.63 to 500 μM and 31.25 to 500 μM, respectively. The procedures were set as follows: 60 s for baseline, 120 s for contact time, and 180 s for the dissociation time at 25 °C. Dissociation constants (K_D) were estimated via associated software (SARTORIUS AG). Moreover, competitive binding to TREM2 was analysed by loading a mixture of BCAAs or BCKAs with Aβ (1 μM), and the binding data for Aβ in the absence of BCAAs or BCKAs were used as a reference.

Immunoprecipitation and LC–MS/MS

The binding of BCAAs and BCKAs to TREM2 in BV2 cells was analysed as previously described [37]. BV2 cells were incubated with the vehicle or isomers of BCAAs or BCKAs (5 mM) at 37 °C for 4 h. After washes with PBS, the cells in homogenization buffer (containing protease inhibitors) were freeze-thawed three times with liquid nitrogen to obtain the lysates. Then, the protein in the cell lysates was acquired by centrifugation at 12,000×*g* for 10 min at 4 °C. Immunoprecipitation was performed using an immunoprecipitation kit with Protein A + G magnetic beads and a rat monoclonal anti-TREM2 antibody (ab125117, Abcam). Immunoprecipitated protein supernatants were collected and heated at 95 °C for 3 min. Then, an adequate amount of methanol (containing 0.1% formic acid) was added to the mixture, the mixture was centrifuged at 12,000×*g* for 10 min at 4 °C, and the precipitate was discarded. Finally, the obtained supernatant was dried under a nitrogen flow and re-dissolved in 100 μL of methanol/deionized water (1:1, v/v, 0.1% formic acid) for LC–MS/MS detection. The standards of isomers of BCAAs and BCKAs were all purchased from MedChemExpress.

Cellular thermal shift assay (CETSA)

The CETSA was performed using a previously described method [39]. BV2 cells were seeded into 6-well plates at 2×10^5 cells per well. The cells were treated with BCAAs or BCKAs (5 mM) for 4 h and harvested in centrifuge tubes. Next, the cell suspensions were divided into 100 μl aliquots and heated at temperatures ranging from 40 to 60 °C for 3 min in a Veriti Fast Thermal Cycler (Thermo Fisher Scientific) with 3 min of cooling. The cell lysate was obtained by undergoing 3 freeze–thaw cycles in homogenization buffer containing protease inhibitors, followed by centrifugation at 12,000×g for 10 min at 4 °C. The supernatant was collected for Western blot analysis.

Cellular TREM2–Aβ binding assay

The binding of Aβ to cellular TREM2 was determined as described in a previous report [23]. BV2 cells were incubated with HiLyte™ Fluor 488-$Aβ_{1–42}$ aggregates in the presence or absence of BCAAs/BCKAs (5 mM) at 4 °C for 2 h. After three washes with cold PBS, the cells were fixed with 4% PFA without permeabilization. TREM2 was labelled with an anti-TREM2 antibody (ab305103, Abcam), and DAPI was used to stain the nuclei. TREM2-bound Aβ was detected using Axio Observer 7 and analysed with ImageJ software.

TREM2 recycling assay

The TREM2 recycling assay was conducted as described previously [33]. First, BV2 cells were treated with BCAAs/BCKAs (5 mM) and Aβ (1 μM) in the presence or absence of the agents rapamycin (50 nM), chloroquine (40 μM) or 4-octyl itaconate (40 μM) for 12 h. The cells were then blocked for 20 min, followed by the addition of an anti-TREM2 antibody (ab305103, Abcam,) diluted in DMEM with 1% foetal bovine serum. After an incubation at 37 °C for 1 h, the cells were washed with prechilled DMEM at pH 2.0 and then cultured in complete medium for 1 h. DyLight 594-labelled secondary antibodies diluted in DMEM with 1% foetal bovine serum were added to the cells, which were incubated for another hour at 37 °C to label recycled TREM2. Next, the cells were washed with prechilled DMEM at pH 2.0 and PBS at pH 7.4 and fixed with 4% PFA for 15 min. DAPI was used to stain the nuclei. The values of recycled TREM2 were quantified as the fluorescence intensity per cell using ImageJ software.

Statistical analysis

All the data are presented as the means ± SEMs. All the statistical analyses were performed using IBM SPSS Statistics 19. The significance of differences was assessed with unpaired Student's t test or one-way or two-way analysis of variance (ANOVA) followed by Tukey's multiple comparisons test, as indicated. The significance threshold was set at $P < 0.05$.

Results

High-fat diet feeding induced obesity and insulin resistance in APP/PS1 mice

APP/PS1 mice, a transgenic mouse model of AD, were used in this study. APP/PS1 mice develop progressive Aβ deposition in the brain at approximately 6 months of age [40] and cognitive deficits from 8–9 months of age [41]. Three-month-old APP/PS1 mice were fed a HFD for 6 months in this study to investigate the effects of a HFD on Aβ pathology and cognitive function. Furthermore, a HFD with adjusted BCAAs contents (100% addition or 50% reduction) was provided to APP/PS1 mice to confirm the role of BCAAs in this progression. Energy intake was not significantly different among the groups (Fig. S1A). Compared with those in the chow group, the APP/PS1 mice in the HFD, HFD + BCAAs and HFD-BCAAs group presented increases in body weight, fasting serum glucose levels, serum insulin levels, and HOMA-IR, as well as impaired glucose tolerance, as indicated by the oral glucose tolerance test (Fig. 1A-C). Increased serum TC and LDL-C levels were also detected in HFD- and HFD with additional BCAAs-fed APP/PS1 mice (Fig. S1B). These results suggested that HFD feeding induced obesity, insulin resistance and lipid metabolism disorders in APP/PS1 mice. However, no significant differences were observed in body weight among the mice in HFD, HFD + BCAAs and HFD-BCAAs groups. Adjusting the BCAAs contents of the HFD had no obvious influence on food intake, insulin resistance and lipid metabolism in APP/PS1 mice compared with those of the HFD-fed mice.

Impaired BCAAs catabolism in HFD-fed APP/PS1 mice

Previous studies have shown that obesity and insulin resistance interrupt BCAAs catabolism in peripheral tissues, which leads to excessive BCAAs accumulation in the circulation [11, 13]. BCAAs are able to cross through the blood–brain barrier via L-type amino acid transporters and maintain the function of the central nervous system [15]. However, the effects of a HFD on BCAAs metabolism in the AD brain remain largely unclear. Here, amino acid levels in the serum and cerebral cortex of APP/PS1 mice were quantified via ultrahigh-performance liquid chromatography tandem mass spectrometry (UPLC-MS/MS). In contrast to those in chow diet-fed mice, the serum levels of leucine, isoleucine, valine and their corresponding metabolites (BCKAs) were elevated in HFD-fed APP/PS1 mice, while differences in the levels of glutamine, lysine, histidine and phenylalanine were observed (Fig. 1D). We further confirmed that HFD feeding triggered the accumulation of corticocerebral BCAAs (except for valine) and BCKAs (Fig. 1E). BCAAs addition or restriction in the HFD altered the concentrations of BCAAs and BCKAs in the serum and cerebral cortex of APP/PS1 mice to different extent. In addition, a positive correlation was detected between the cortical levels and the circulating levels (Fig. 1F). The relative abundances of other amino acids in the cortex are listed in Fig. S1C.

Then, we measured the protein levels of BCAAs metabolic enzymes in peripheral tissues and the brain. Two key enzymes, branched-chain aminotransferase (BCAT) and BCKAs dehydrogenase (BCKDH), are involved in BCAAs catabolism. BCAAs are transformed into BCKAs in a reversible transamination reaction facilitated by BCAT. Subsequently, BCKDH conducts the irreversible decarboxylation of BCKAs, which is a rate-limiting step in BCAAs catabolism. Phosphorylation of the BCKD E1α subunit by BCKD kinase (BCKDK) inhibits the activity of BCKDH [42, 43]. As presented in Fig. 1G and H, the protein levels of BCAT2 in the liver and skeletal muscle of HFD-fed mice remained unchanged compared with those of chow-fed mice, whereas the phosphorylation ratio of BCKDH was increased by the overexpression of BCKDK. Moreover, the IHC results demonstrated that HFD feeding reduced BCAT2 protein levels in the hippocampus and cerebral cortex (Fig. S1D and E), and

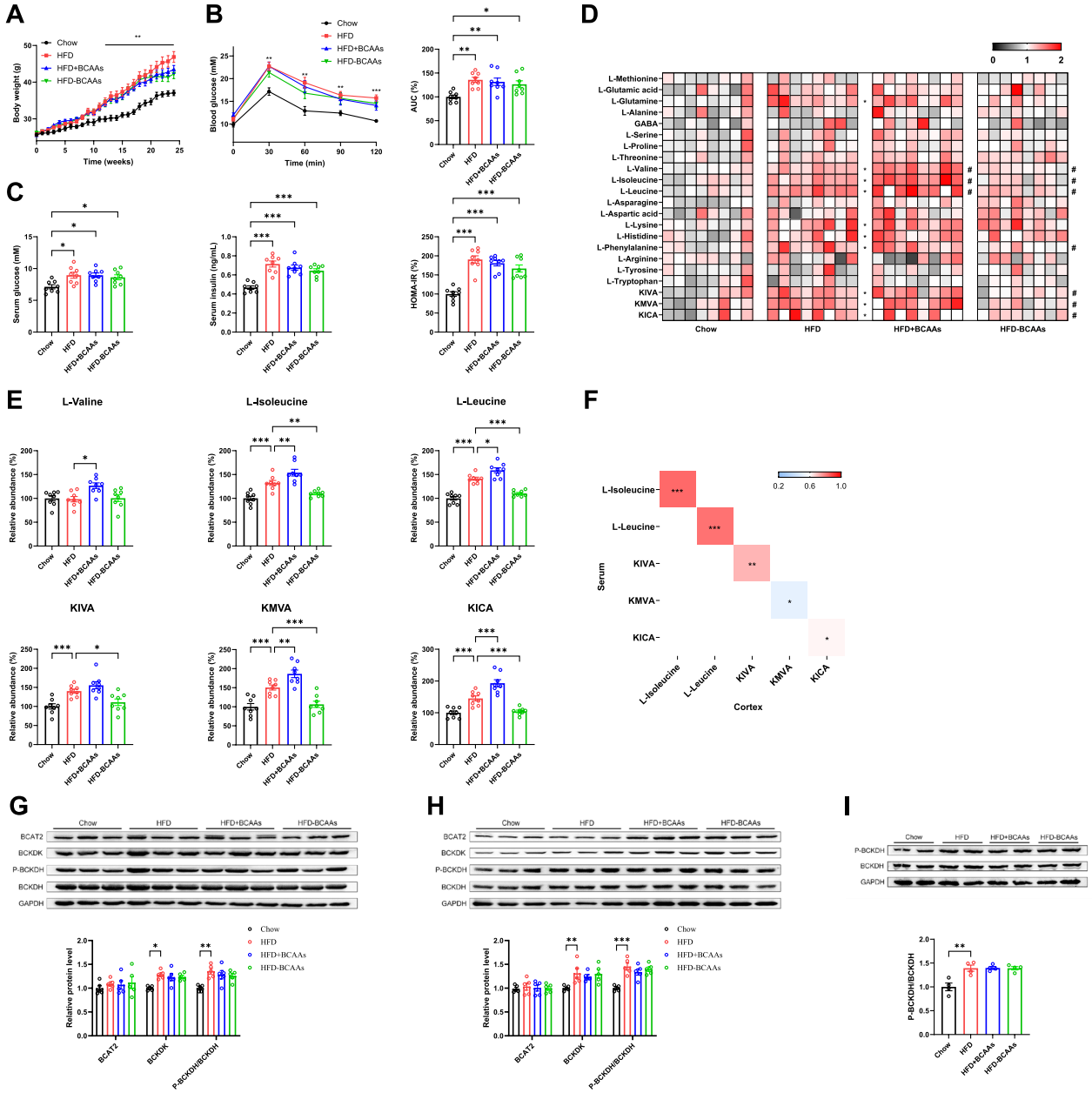

Fig. 1 HFD feeding induces insulin resistance and disruptes BCAAs catabolism in APP/PS1 mice. **A** Body weight of APP/PS1 mice during experiment period (n = 11 to 12). **B** Blood glucose levels in the glucose tolerance test (OGTT) and the area under the curve (AUC) of APP/PS1 mice (n = 8). **C** Fasting serum glucose and insulin levels, and corresponding HOMA-IR index of APP/PS1 mice (n = 8). **D** Heatmaps of the amino acid levels in serum of APP/PS1 mice in the indicated groups (n = 8). **E** Comparison of the levels of BCAAs and BCKAs in cerebral cortex (n = 8). **F** Heatmap analysis of the Spearman correlation of circulating and cortical levels of BCAAs and BCKAs. Western blot analysis of the levels of BCAAs catabolism-related protein in liver (**G**), skeletal muscle (**H**), and cerebral cortex (**I**), and the corresponding quantification results (n = 4–5). Data are means ± SEM. *P < 0.05,**P < 0.01 and ***P < 0.001, two-way or one-way ANOVA, followed by Tukey's multiple comparisons test

hyperphosphorylation of BCKDH in the cerebral cortex was revealed by Western blotting (Fig. 1I). These results indicated the suppression of BCAAs catabolism in peripheral and cerebral tissues after HFD feeding, which was not affected by the adjustment of the BCAAs concentration in the HFD. In summary, we discovered that a HFD impairs BCAAs metabolism, resulting in the accumulation of BCAAs and BCKAs in the serum and cerebral cortex of APP/PS1 mice. The increased levels of BCAAs and BCKAs in the cerebral cortex are not

only related to the inhibition of BCAAs degradation in the brain but also are related to increased levels in the circulation.

The accumulation of BCAAs and BCKAs exacerbates cognitive deficits and AD-related pathology in HFD-fed APP/PS1 mice

A number of studies have reported that a HFD promotes cognitive deficits and AD-related pathology during AD development through metabolic disorders [7, 44]. Nevertheless, whether HFD-induced BCAAs metabolism disorders participate in this progression has not yet been confirmed. Thus, we tested the spatial learning and memory of APP/PS1 mice using the Morris water maze and evaluated AD-related pathology by performing immunofluorescence staining and Western blotting. As displayed in Fig. 2A to E, APP/PS1 mice in the HFD group performed poorer in the Morris water maze test than those in the chow group did, which was supported by longer escape latency times during the training trials, as well as fewer entries into the target platform location and target quadrants in the probe trial. Importantly, additional intake of BCAAs further aggravated spatial learning and memory deficits; in contrast, limitation of BCAAs reversed these defects in HFD-fed mice. The swimming speed of the mice did not affect these phenotypes in the different groups. In addition, BCAAs and BCKAs levels in the cerebral cortex were negatively associated with the cognitive function of APP/PS1 mice (Fig. 2F).

Cognitive deficits are usually accompanied by presence of AD-related pathology, including synaptic degeneration and Aβ pathology in AD, which reflects disease progression [45]. In accordance with the trend in cognitive deficits, the Western blot results indicated that HFD feeding markedly decreased the levels of synaptophysin and PSD95 (pre- and postsynaptic markers, respectively) in the cortices compared to chow diet feeding (Fig. 2G), revealing synaptic impairments in the brains of HFD-fed APP/PS1 mice. Compared with HFD feeding, adding or reducing the BCAAs contents of the HFD deteriorated or alleviated the postsynaptic impairment in the cerebral cortex, respectively. Moreover, restriction of BCAAs also rescued the presynaptic impairment, as indicated by increased levels of synaptophysin. Substantial evidence suggests that the synaptic impairment occurs later than Aβ accumulation during AD development [46, 47]. According to the immunofluorescence results obtained with a specific antibody, greater Aβ deposition was observed in the brains of mice in the HFD group than in mice in the chow group (Fig. 2I). The Aβ burden in HFD-fed mice was increased or decreased by BCAAs addition or restriction, respectively. The ELISA results of total $A\beta_{1-40}$ and $A\beta_{1-42}$ showed similar trends with the immunofluorescence results (Fig. S2A and B). However, no significant differences in the protein levels of the APP and APP processing secretase (BACE1) in the cerebral cortex were detected among all the groups, suggesting that Aβ production remained unchanged (Fig. 2H and Fig. S2C). Taken together, these findings suggest that accumulated BCAAs and BCKAs promote the HFD-induced development of cognitive deficits, synaptic degeneration and Aβ pathology in APP/PS1 mice.

Excessive BCAAs and BCKAs lead to dysregulated microglial clearance of Aβ

Aβ accumulation and aggregation are commonly attributed to an imbalance in Aβ production and clearance [48]. Because Aβ production was not altered in the animals used in this study, we hypothesized that BCAAs exacerbated the Aβ burden by reducing Aβ clearance. Microglia are able to conduct phagocytosis and clearance of extracellular Aβ in the brain [25, 33]. Although previous studies have shown that excessive BCAAs impact microglial polarization and inflammation, whether BCAAs hinder Aβ clearance by dysfunctional microglia is unknown [27, 28]. First, we analysed the number of microglia in the brains of the mice with an anti-IBA1 (a microglial marker) antibody. The immunofluorescence results revealed greater microglial accumulation in the brains of HFD-fed APP/PS1 mice than in those of chow diet-fed APP/PS1 mice, which was also confirmed by the increased IBA1 levels detected via Western blotting (Fig. 3A and B). The number of microglia recovered as a result of BCAAs-restricted diet feeding. Then, microglia and Aβ plaques were colabelled with anti-IBA1 and anti-Aβ antibodies in the brains of mice. The IBA1 + cells around plaques indicates the microglial recruitment and response to Aβ plaques, which reflects microglial phagocytic capacity of Aβ to some extent [25, 36]. As presented in Fig. 3C, the number of microglia around Aβ plaques in the cortex and hippocampus was reduced after HFD feeding. In contrast to HFD feeding, additional BCAAs intake further restrained the clustering of microglia surrounding Aβ plaques. Conversely, the number of microglia around Aβ plaques was increased in BCAAs-restricted diet-fed mice. These results suggested that HFD feeding impaired microglial recruitment and response to Aβ plaques, which possibly decreased microglial phagocytosis of Aβ in the brain. Accumulation of BCAAs and BCKAs might also participate in this progression, and restriction of BCAAs intake restored the microglial response to Aβ plaques.

Mouse microglia BV2 cells were used to determine whether excessive BCAAs and BCKAs could suppress Aβ phagocytosis or degradation in microglia. After BCAAs or BCKAs treatment, fluorescein labelled-Aβ

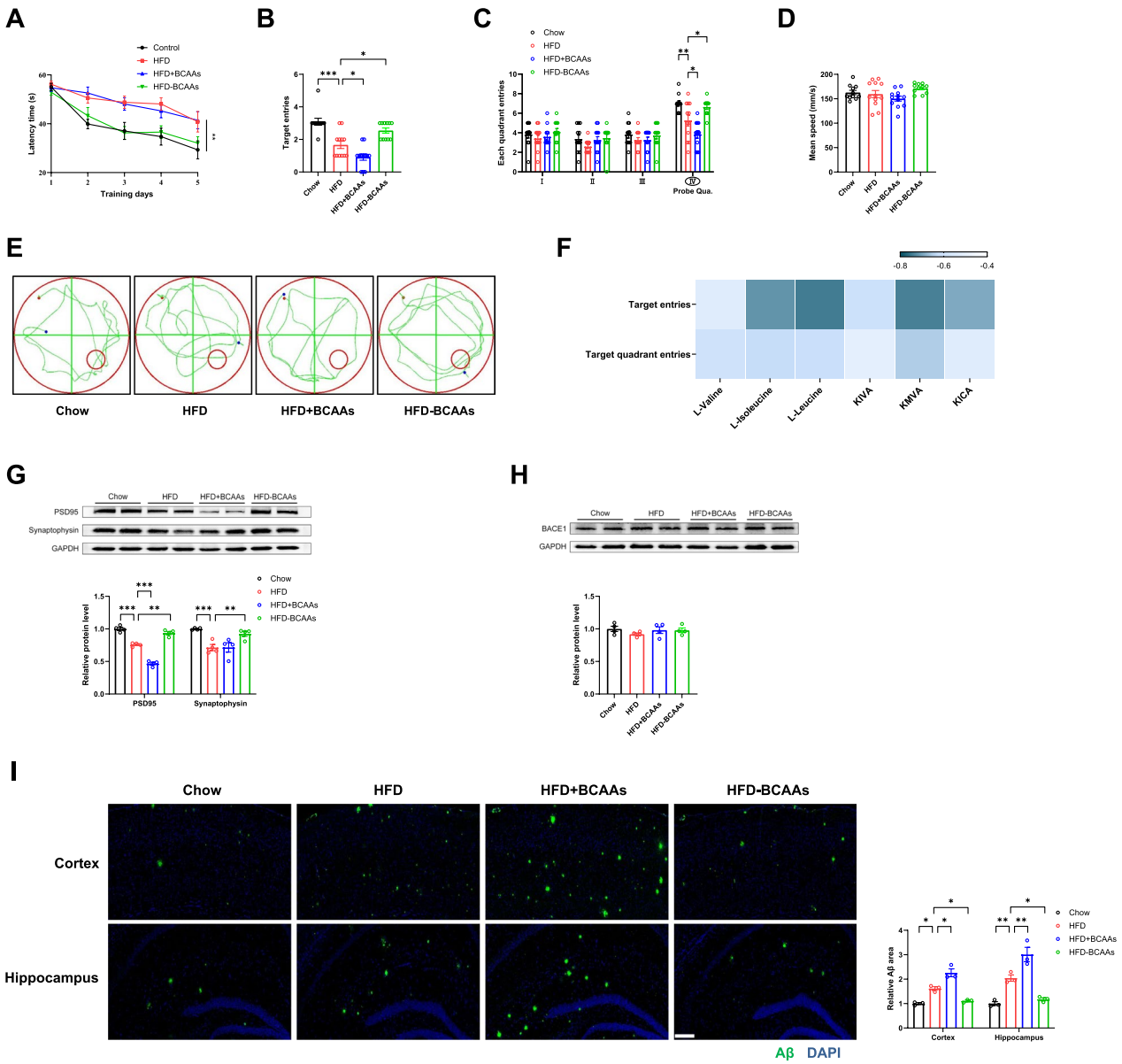

Fig. 2 BCAAs addition and restriction affect the development of cognitive deficits and AD-related pathology in HFD-fed APP/PS1 mice. **A** Escape latency to the platform during the training trails in a Morris water maze (n = 11 to 12). **B** Target (platform) entries in the probe test (n = 11 to 12). **C** Target quadrant entries in the probe test (n = 11 to 12). **D** Mean swimming speed of mice (n = 11 to 12). **E** Representative swimming tracks of mice in the probe test (n = 11 to 12). (F) Heatmap analysis of the Spearman correlation of cognitive function-related indexes and cortical levels of BCAAs and BCKAs (n = 8). **G** Western blot analysis of the protein levels of postsynaptic (PSD95) and presynaptic (synaptophysin) markers in cerebral cortex of mice, and the corresponding quantification results (n = 4). (H) Western blot analysis of the protein levels of Aβ secretase (BACE1) in cerebral cortex and the corresponding quantification results (n = 4). **I** Immunostainings of Aβ plaques by using specific antibody (6E10) in cortex and hippocampus (Scale bars, 200 μm), and quantitation of positive area rate (n = 3). Data are means ± SEM. *P < 0.05,**P < 0.01 and ***P < 0.001, two-way or one-way ANOVA, followed by Tukey's multiple comparisons test

uptake by microglia was markedly decreased, as evidenced by the decreased fluorescence intensity at 4–12 h (Fig. 3D). However, no obvious difference in Aβ degradation was observed between the control and BCAAs- or BCKAs-treated cells (Fig. 3E). In summary, elevated BCAAs and BCKAs levels inhibited the Aβ phagocytic activity of microglia, thereby disturbing Aβ clearance, but the underlying mechanisms need to be further elucidated.

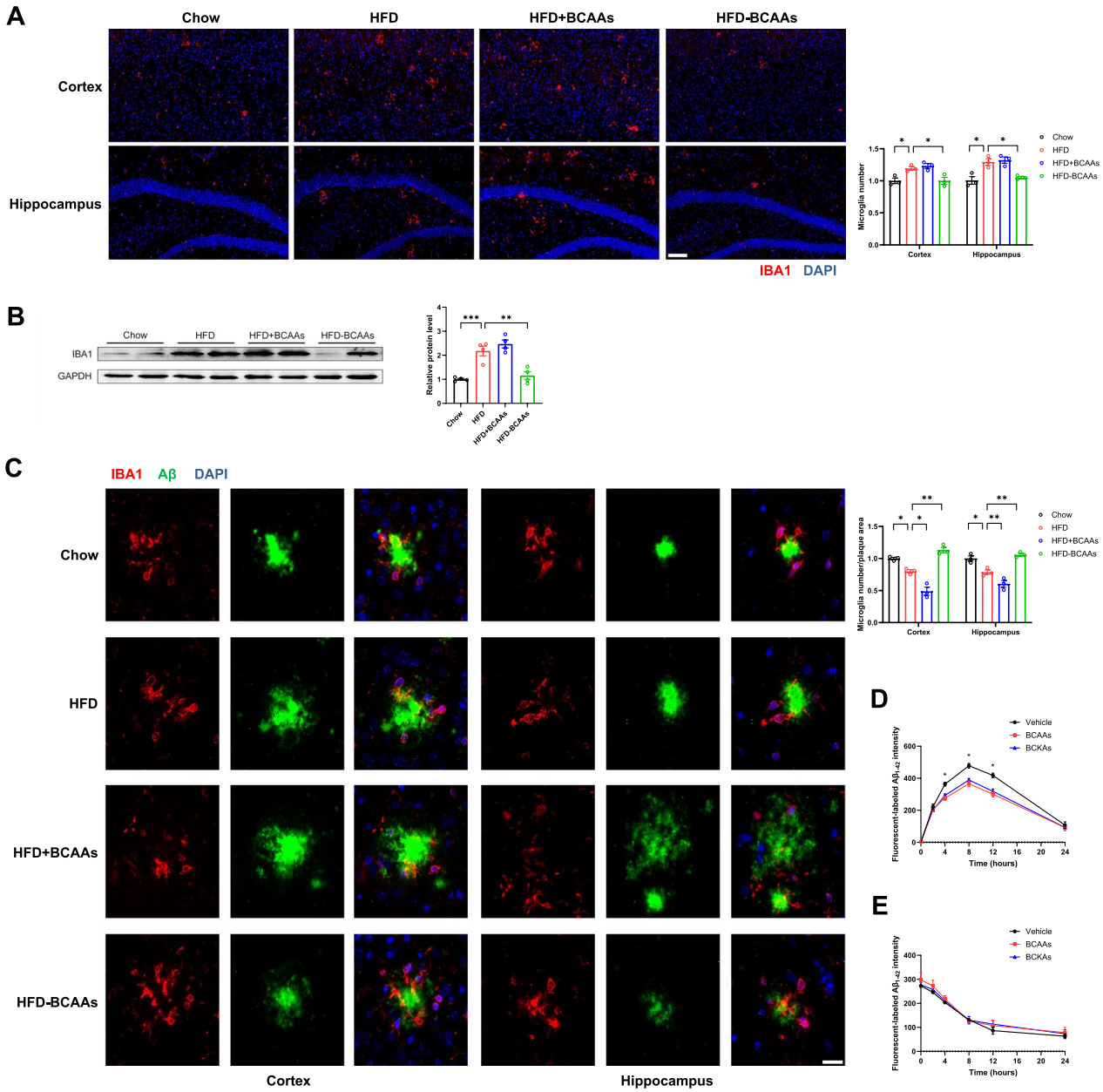

Fig. 3 BCAAs and BCKAs contribute to microglial phagocytosis deficiency in HFD-fed APP/PS1 mice and BV2 cell. **A** Representative images of microglia (IBA1) staining in cortex and hippocampus of APP/PS1 mice (Scale bars, 100 μm), and corresponding quantitation of positive cell number (n = 3). **B** Western blot analysis of IBA1 levels in cortex, and the corresponding quantification results (n = 4). **C** Representative images of Aβ plaques (6E10) and microglia (IBA1) co-staining in cortex and hippocampus of APP/PS1 mice (Scale bars, 20 μm), and corresponding quantitation of positive cell number around plaque (n = 3). Microglial phagocytosis **D** and degradation **E** of fluorescein labeled-Aβ for the indicated time in BV2 cells in the presence or absence of BCAAs/ BCKAs (n = 3). Data are means ± SEM. *P < 0.05,**P < 0.01 and ***P < 0.001, one-way ANOVA, followed by Tukey's multiple comparisons test

BCAAs and BCKAs suppress the response of TREM2 and autophagy to Aβ in microglia

Next, we investigated how BCAAs and BCKAs affect Aβ phagocytosis by microglia. Recently, TREM2, a transmembrane receptor activated by extracellular Aβ, has been reported to be critical for the microglial response to Aβ [25]. Meanwhile, microglial autophagy facilitates the clearance of Aβ [22, 32]. BCAAs and BCKAs act as mTORC1 activators to block autophagic activity [49], and an autophagy deficiency is considered to lead to TREM2 dysregulation [33]. Here, the mRNA and protein levels of TREM2 and autophagy-related markers in the cortex of

APP/PS1 mice were analysed by QPCR and Western blotting, respectively. As shown in Fig. 4A, compared with chow diet feeding, HFD feeding reduced the phosphorylation of SYK without altering TREM2 levels in APP/PS1 mice, indicating the inhibition of TREM2 activation. Compared with that in HFD-fed mice, the TREM2 protein level in HFD-fed mice decreased with increasing BCAAs intake, while the phosphorylation of SYK was further suppressed. On the other hand, restriction of BCAAs intake restored TREM2 activation. Moreover, the mRNA levels of the TREM2-related protein DAP12 and the phagosome marker CD68 were decreased in the HFD + BCAAs group (Fig. 4B). Additionally, mTORC1 was activated and autophagic activity was lower in the cortex of the mice in the HFD group than in those in the chow group, as suggested by the increased levels of the phosphorylated S6K protein and the P62 protein, a decrease in the conversion of LC3-I to LC3-II, and decreases in the mRNA levels of BECLIN1 and LAMP1 (Fig. 4C and D). The addition or reduction in BCAAs

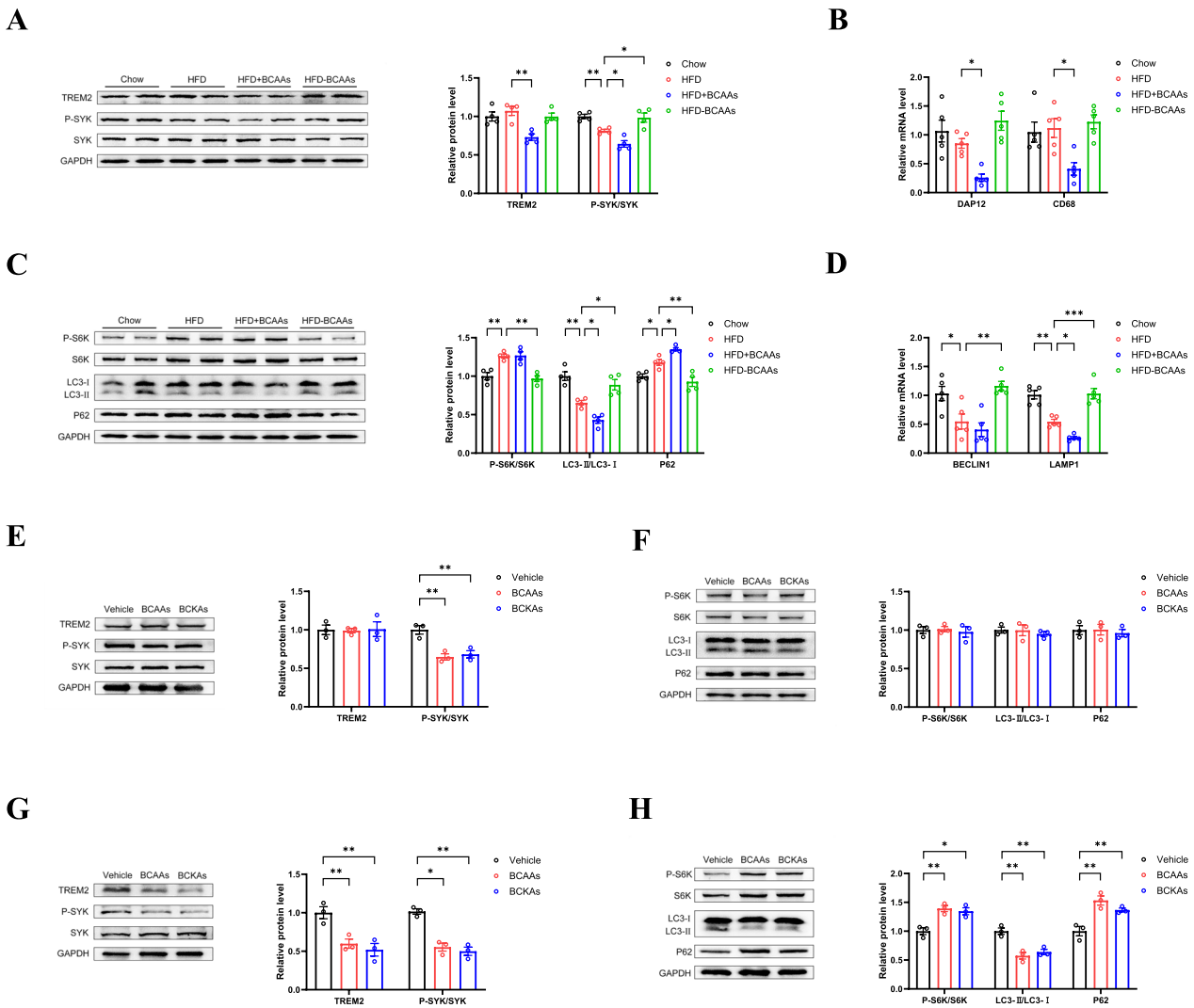

Fig. 4 BCAAs and BCKAs impact the response of microglial TREM2 and autophagy to Aβ. **A** Western blot analysis of TREM2-related protein levels in cortex of APP/PS1 mice and the corresponding quantification results (n = 4). **B** Relative mRNA levels of DAP12 and CD68 in cortex (n = 5). **C** Western blot analysis of autophagy-related protein levels in cortex and the corresponding quantification results (n = 4). **D** Relative mRNA levels of BECLIN1 and LAMP1 in cortex (n = 5). Western blot analysis of TREM2-related **E** and autophagy-related **F** Protein levels in BV2 cell treated with or without BCAAs/ BCKAs for 4 h in the presence of Aβ and the corresponding quantification results (n = 3). Western blot analysis of TREM2-related **G** and autophagy-related **H** protein levels in BV2 cell treated with or without BCAAs/ BCKAs for 12 h in the presence of Aβ and the corresponding quantification results (n = 3). Data are means ± SEM. *P < 0.05,**P < 0.01 and ***P < 0.001, one-way ANOVA, followed by Tukey's multiple comparisons test

contents in the HFD had opposite effects on autophagy in the cortex of APP/PS1 mice.

Previously, we reported that Aβ phagocytosis by BV2 cells changed with the BCAAs or BCKAs intervention from 4 to 12 h. We determined whether TREM2 and autophagy were involved in the effects of BCAAs and BCKAs on microglial Aβ phagocytosis by treating BV2 cells with Aβ and BCAAs/BCKAs for 4 h and 12 h, followed by Western blot analysis. The results revealed that the response of TREM2 to Aβ was blunted in BV2 cells upon BCAAs or BCKAs treatment for 4 h, but no alterations in autophagy or TREM2 protein levels were detected (Fig. 4E and F). After treating BV2 cells for 12 h, BCAAs or BCKAs resulted in an autophagy deficiency and the downregulation of TREM2 protein levels (Fig. 4G and H).

BCAAs and BCKAs bind to TREM2, thereby depressing microglial TREM2 activation

Aβ is able to bind to the TREM2 extracellular domain, which stimulates TREM2 activation to initiate the microglial phagocytosis of Aβ [23, 29]. Combined with the results that BCAAs and BCKAs inhibited TREM2 activation in response to Aβ without changing TREM2 protein levels, we hypothesized that BCAAs and BCKAs disrupted microglial TREM2 function possibly through direct binding to TREM2. We tested this hypothesis using molecular docking to investigate the potential interaction between TREM2 and BCAAs/BCKAs. The predicted results revealed that all three BCAAs and three BCKAs could interact with the TREM2 extracellular domain, and the affinity ranged from −3.8 to 4.1 kcal/mol (Fig. 5A and Fig. S3A). L-leucine and its metabolite KICA were used as examples; L-leucine and KICA can form key hydrogen bonds with ASP104 [37], and other amino acid residues, such as THR82, TYR108, ARG52, and VAL62, also participate in the interaction. The binding of BCAAs and BCKAs to TREM2 was subsequently explored via biolayer interferometry (BLI). The shift in the spectra was enhanced (Fig. 5B) by the gradual increase in the concentration of ligands, revealing that both BCAAs and BCKAs bound to the TREM2 protein in solution. Next, we treated BV2 cells with an isotope of BCAAs or BCKAs (to avoid noise from the substrate), followed by immunoprecipitation combined with LC–MS/MS. BCAAs isotope treatment led to the occurrence of corresponding peaks in the LC–MS/MS spectra (Fig. 5C and Fig. S3B). Unfortunately, the BCKAs content in the immunoprecipitate was too low to be detected, which might be due to the low signal intensity of the standards in LC–MS/MS (data not shown). In addition, CETSA revealed that treating BV2 cells with BCAAs or BCKAs stabilized the TREM2 protein during heat challenge (Fig. 5D). These results illustrated that BCAAs and BCKAs interact with TREM2 in the cellular environment. Competition experiments were performed using BLI and immunofluorescence staining to examine whether this interaction influences the response of TREM2 to Aβ. As presented in Fig. S3C, BCAAs and BCKAs constrained the binding of Aβ to TREM2, as supported by the reduction in the spectral shift in the BLI assay. In addition, the level of Aβ surrounding TREM2 in BV2 cells decreased in the presence of BCAAs or BCKAs (Fig. 5E). Finally, we found that treatment with S1P, a TREM2 ligand that promotes microglial phagocytosis [37], reversed the BCAAs/BCKAs-induced repression of Aβ uptake and TREM2 activation in BV2 cells (Fig. 5F and G), which further confirmed that BCAAs and BCKAs reduced the microglial phagocytosis of Aβ by binding to TREM2.

BCAAs and BCKAs reduce the expression and recycling of microglial TREM2 via autophagy

Our previous results suggested that BCAAs and BCKAs treatment for 12 h reduced TREM2 protein levels in BV2 cells, accompanied by an autophagy deficiency. In addition, recycled TREM2 supports the clearance of Aβ deposits, and autophagy-related proteins are functionally involved in TREM2 recycling [33]. Thus, we hypothesized that BCAAs and BCKAs decrease the expression and recycling of microglial TREM2 through the inhibition of autophagy. First, the mTOR inhibitor rapamycin was used to explore the effects of autophagy on TREM2. The Western blot results revealed that rapamycin treatment restored TREM2 function and promoted autophagy in BV2 cells in the presence of BCAAs/BCKAs, as indicated by increased protein levels of TREM2 and phosphorylation of SYK, as well as decreased phosphorylation of S6K and protein levels of P62 (Fig. 6A and B). Moreover, the decreased phagocytosis of fluorescein labelled-Aβ42 in BV2 cells was reversed by rapamycin (Fig. 6C). Unexpectedly, although both BCAAs and BCKAs decreased TREM2 recycling in BV2 cells, no obvious change in TREM2 recycling was detected after rapamycin treatment compared with treatment with BCAAs/BCKAs without rapamycin (Fig. 6D). As mTOR-independent nonclassical autophagy is critical for TREM2 recycling, the nonclassical autophagy activators chloroquine and 4-octyl itaconate (4-OIC) were used to further determine how BCAAs/BCKAs influence TREM2 recycling [50–52]. As shown in Fig. 6E, F and G, increased protein levels of TREM2 and LC3-II/LC3-I were observed in BV2 cells after chloroquine treatment, whereas the BCAAs/BCKAs-induced decrease in TREM2 recycling was reversed. However, mTOR activity and P62 accumulation in BV2 cells were not altered by chloroquine. Similarly, 4-OIC treatment increased the levels of RUBICON and

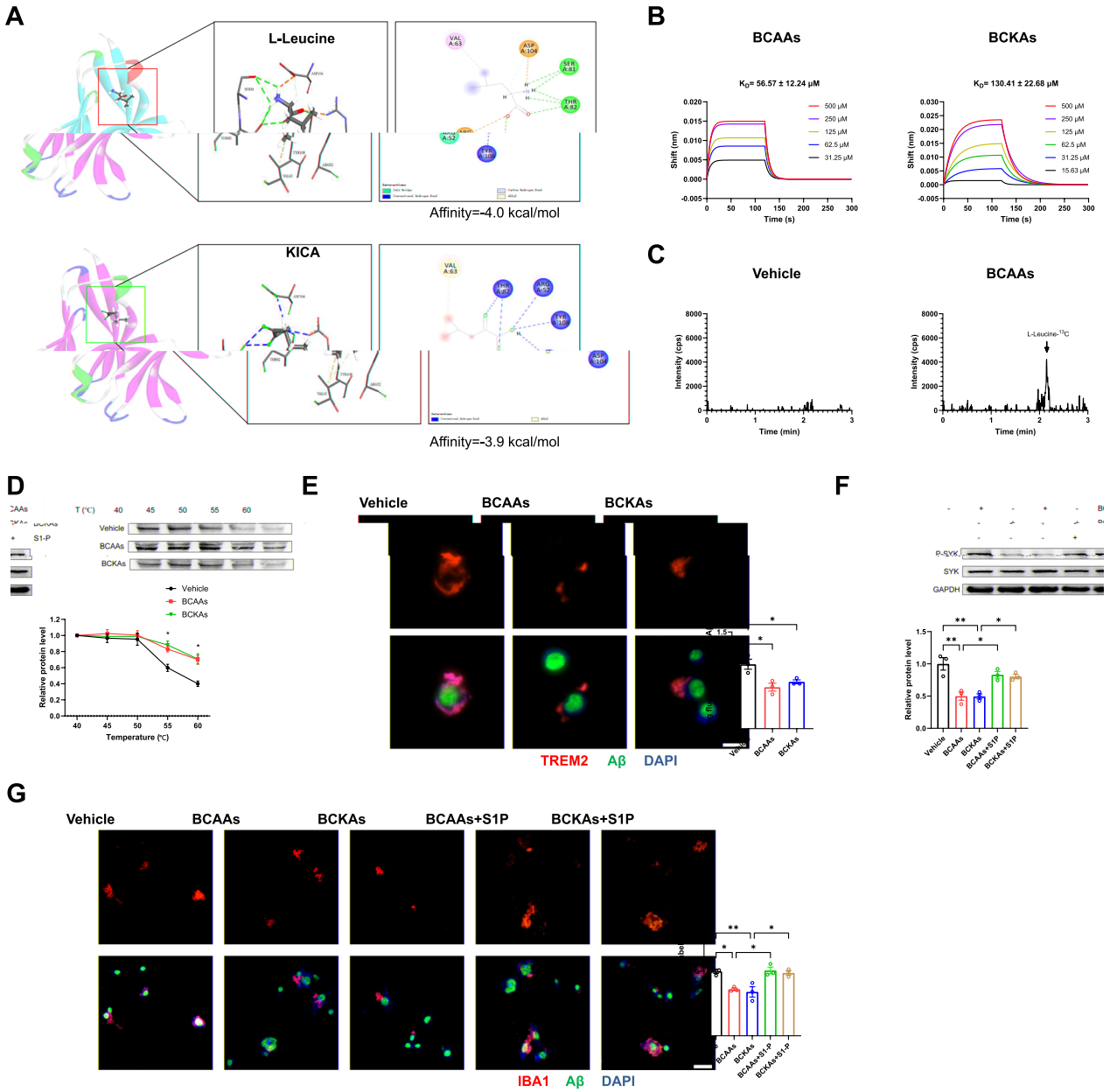

Fig. 5 BCAAs and BCKAs suppress TREM2 activation through binding to TREM2. **A** Molecular docking results of L-Leucine and KICA binding to TREM2 extracellular domain. **B** Biolayer interferometry (BLI) analysis of interaction of BCAAs or BCKAs with TREM2. BCAAs and BCKAs was titrated from 15.63 to 500 μM and 31.25 to 500 μM, respectively. **C** LC–MS/MS spectra of TREM2 immunoprecipitated L-Leucine-^{13}C of BV2 cells after BCAAs isotope treatment for 1 h. **D** Thermal stabilization of TREM2 protein evaluated by cellular thermal shift assay (CETSA) after treating BV2 cells with BCAAs/ BCKAs for 4 h (n = 3). **E** Representative images of binding of fluorescein labeled-Aβ to cell surface TREM2 in BV2 cells after treatment of BCAAs/ BCKAs for 2 h (n = 3, Scale bars, 40 μm). **F** Representative images of microglial phagocytosis of fluorescein labeled-Aβ in BV2 cells after treatment of BCAAs/ BCKAs in the presence or absence of S1P for 4 h (n = 3, Scale bars, 40 μm). **G** Western blot analysis of phosphorylation levels of SYK in BV2 cell after treatment of BCAAs/ BCKAs in the presence or absence of sphingosine-1-phosphate (S1P) for 4 h (n = 3). Data in **D**, **E**, **F** and **G** are means ± SEM. *P < 0.05,**P < 0.01 and ***P < 0.001, one-way ANOVA, followed by Tukey's multiple comparisons test

LC3-II/LC3-I with increased TREM2 recycling in BV2 cells (Fig. S4A and B). Additionally, both chloroquine and 4-OIC were able to rescue microglial uptake of Aβ in the presence of BCAAs/BCKAs (Fig. S4C). These results indicate that BCAAs/BCKAs affect TREM2 expression in an mTOR-dependent manner and affect TREM2 recycling in an mTOR-independent LC3 lipidation-dependent manner.

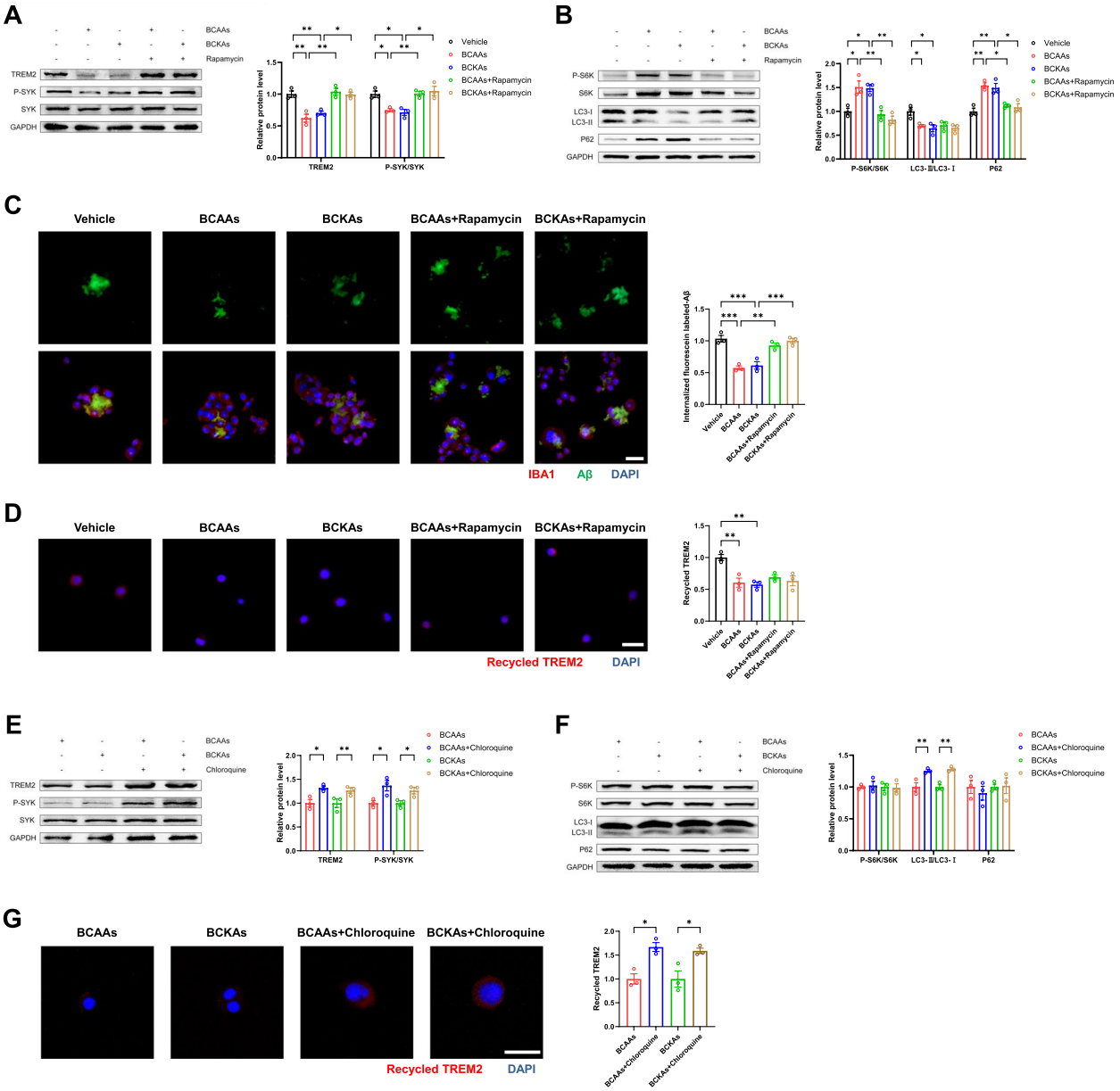

Fig. 6 BCAAs and BCKAs reduce the expression and recycling of microglial TREM2 via inhibiting autophagy. Western blot analysis of TREM2-related **A** and autophagy-related **B** protein levels in BV2 cell after treatment of BCAAs/ BCKAs in the presence or absence of rapamycin for 12 h (n = 3). **C** Representative images of microglial phagocytosis of fluorescein labeled-Aβ in BV2 cells after treatment of BCAAs/ BCKAs in the presence or absence of rapamycin for 12 h (n = 3, Scale bars, 40 μm). **D** Representative images of TREM2 recycling in BV2 cells after treatment of BCAAs/ BCKAs in the presence or absence of rapamycin for 12 h (n = 3, Scale bars, 40 μm). Western blot analysis of TREM2-related **E** and autophagy-related **F** protein levels in BV2 cell after treatment of BCAAs/ BCKAs in the presence or absence of chloroquine for 12 h (n = 3). **G** Representative images of TREM2 recycling in BV2 cells after treatment of BCAAs/ BCKAs in the presence or absence of chloroquine for 12 h (n = 3, Scale bars, 40 μm). Data are means ± SEM. *P < 0.05,**P < 0.01 and ***P < 0.001, one-way ANOVA, followed by Tukey's multiple comparisons test or Student's t test

Discussion

Numerous studies have revealed a pathophysiological association between T2DM and AD [2, 3]. A HFD potentially accelerates the development of AD through various pathways [8]. A HFD results in complex metabolic disturbances, including insulin resistance and obesity, which are related to T2DM. Epidemiological and experimental studies indicate that insulin resistance and obesity lead to BCAAs accumulation by impairing BCAAs catabolism [11–13]. Nevertheless, whether excessive

BCAAs are involved in the HFD-induced exacerbation of AD remain largely unclear. Here, we report that excessive BCAAs and BCKAs are linked to HFD-induced AD progression in APP/PS1 mice. In terms of mechanisms, BCAAs and BCKAs can influence TREM2 function, thereby interfering with the microglial clearance of Aβ.

Aβ deposition in the brain has been hypothesized to drive the pathogenic cascades of AD [6]. APP/PS1 mice, an AD model featuring Aβ pathology, typically develop cognitive deficits from 8–9 months of age [41, 53]. Three-month-old APP/PS1 mice were fed a HFD for 6 months in this study to investigate the pathology in the early stage of AD. HFD feeding induced obesity and insulin resistance in APP/PS1 mice. Additionally, BCAA catabolism was inhibited in the peripheral and cerebral tissues of HFD-fed mice, which caused BCAAs and BCKAs accumulation in the circulation and cortex. BCAAs maintain the nitrogen balance and participate in various biological processes in the brain [14]. However, elevated levels of BCAAs and their metabolite BCKAs are neurotoxic and disrupt the normal physiological functions of the brain [15]. In this study, HFD feeding aggravated cognitive deficits, synaptic plasticity impairments and Aβ pathology in APP/PS1 mice. In addition, adjusting the BCAAs contents of the HFD influenced the BCAAs and BCKAs levels without obvious changes in obesity, insulin resistance or BCAAs catabolism. The additional intake of BCAAs further deteriorated cognitive function, cognitive deficits and AD-related pathology in HFD-fed mice. On the other hand, the restriction of BCAAs intake delayed AD progression. These results confirmed the role of BCAAs in the HFD-induced exacerbation of AD.

Microglia, the primary immune cells of the central nervous system, are the cells responding to Aβ accumulation [21]. An abnormal phagocytic capacity of microglia results in reduced Aβ clearance, which eventually contributes to late-onset AD [25]. Previous studies have indicated that BCAAs influence the immune properties of microglia in response to lipopolysaccharide (LPS) [27, 28]. Here, we found that adjusting BCAA intake affected the microglial response to Aβ in vivo and that BCAAs or BCKAs dramatically hindered Aβ phagocytosis in BV2 cells. However, no effects of BCAAs or BCKAs on Aβ degradation in BV2 cells were observed, while the autophagy of BV2 cells was inhibited. A previous study suggested that ablation of autophagy-related proteins (ATG5 or FIP200) resulted in autophagy deficiency but did not affect Aβ degradation in microglia [33]. The unchanged microglial Aβ degradation in our study might be related to other pathways of Aβ degradation apart from autophagy. It is reported that TREM2, the receptor in microglia, conducts microglial phagocytosis of Aβ [23]. TREM2 variants, deficiency or hypofunction lead to the accelerated development of AD [25, 26]. Recently, HFD feeding was shown to induce TREM2 hypofunction in mice [18, 20]. Moreover, BCAAs inhibit autophagic activity through the mTOR pathway, and autophagy also participates in the maintenance of TREM2 function [22, 33]. However, the exact role of BCAAs in regulating TREM2 function remains unknown. In the present study, HFD feeding impaired TREM2 activation without altering TREM2 protein levels in the cortex of APP/PS1 mice, which was reversed by BCAAs restriction. Additionally, excessive BCAAs intake reduced TREM2 protein levels, accompanied by the aggravation of HFD-induced autophagy deficits. In vitro, BCAAs- or BCKAs-treated BV2 cells presented a blunted TREM2 response to Aβ, with unchanged TREM2 protein levels and autophagic activity after 4 h, as well as decreased TREM2 protein levels and autophagy defects after 12 h. Next, we discuss the molecular mechanisms underlying these phenomena.

The findings from BV2 cells after treatment for 4 h are characteristic of molecular binding-induced effects. TREM2 has several potential ligands, including apolipoproteins, phospholipids, the platinum (IV) complex, and Aβ [29, 54]. Among them, Aβ activates TREM2 by binding to the TREM2 extracellular domain and initiates microglial phagocytosis [23, 55]. Our computer simulation and BLI results indicated that BCAAs and BCKAs could bind to the TREM2 protein. Next, the binding of BCAAs and BCKAs to TREM2 in the cellular environment was further confirmed using immunoprecipitation combined with LC–MS/MS and CETSA, which are methods used to explore the interactions between ligands and proteins in cells [37, 56]. In addition, BCAAs and BCKAs competed with Aβ for TREM2 binding in BLI and cell experiments. Treatment with S1P, an agonist that binds to TERM2 and promotes microglial phagocytosis [37], restored the Aβ intake of BV2 cells in the presence of BCAAs or BCKAs, suggesting that BCAAs and BCKAs can bind to TREM2, thereby decreasing microglial phagocytosis of Aβ. A HFD causes multiple metabolic abnormalities, and whether other metabolites are able to bind with TREM2 in a similar manner remains unknown.

After treatment with BCAAs or BCKAs for 12 h, abnormal TREM2 expression and autophagy were detected in BV2 cells. With respect to the relationship between autophagy and TREM2, the evidence indicates that autophagy in microglia is increased in response to Aβ and that hypofunctional microglial autophagy leads to the downregulation of TREM2 in the brains of AD mice [22, 32]. In this study, rapamycin treatment reactivated autophagy and restored TREM2 protein levels and Aβ phagocytosis in BV2 cells in the presence of BCAAs or BCKAs. Nonetheless, the recycling of TREM2 was

not improved in rapamycin-treated BV2 cells, indicating that BCAAs or BCKAs affected recycling of TREM2 in an mTOR-independent manner. Earlier report showed that RUBICON- and ATG5-dependent noncanonical autophagy (LC3-associated endocytosis) is required for TREM2 recycling in microglia, which supports the clearance of Aβ [33]. In order to investigate whether noncanonical autophagy was involved, chloroquine and 4-OIC were used to activate noncanonical autophagy. Chloroquine, known as a lysosomotropic agent, can promote LC3 lipidation independently from canonical autophagy and activate the noncanonical autophagy. The LC3 lipidation induced by chloroquine is associated with endolysosomal membranes during noncanonical autophagy, but it is not associated with autophagosomes [51, 57]. Moreover, the activation of NRF2 can trigger noncanonical autophagy by increasing RUBICON expression [52], and the NRF2 activator 4-OIC can increase microglial phagocytosis [58]. Here, we found that both chloroquine and 4-OIC reversed the suppression of TREM2 recycling and Aβ intake induced by BCAAs or BCKAs, accompanied by increases in LC3 lipidation, revealing that BCAAs and BCKAs inhibit TREM2 recycling possibly through the noncanonical autophagy pathway. However, the exact molecular mechanisms underlying the effects on TREM2 recycling need to be further confirmed.

Conclusions

Our results suggest that accumulated BCAAs and their metabolites BCKAs promote the HFD-induced aggravation of AD in the early pathological stage. BCAAs and BCKAs disrupt the microglial phagocytosis of Aβ via dysfunctional TREM2, in which binding to TREM2 and autophagy are possibly involved. This evidence provides a theoretical basis for understanding the relationship between diet-induced metabolic abnormalities and AD progression, and the dietary preventive interventions for AD. As prospects, inhibitors that target BCKDK (such as BT2) to effectively lower BCAAs levels [13, 52] have the potential to serve as promising pharmacological strategies for AD in the future.

Supplementary Information

The online version contains supplementary material available at https://doi.org/10.1186/s12974-024-03314-1.

Supplementary Material 1

Supplementary Material 2

Author contributions

Yang Yang: Investigation, Data curation, Visualization, Methodology, Validation, Writing – original draft. Guanjin Shi: Investigation, Methodology, Data curation. Yanyan Ge: Data curation, Methodology. Shanshan Huang: Data curation, Methodology. Ningning Cui: Methodology. Le Tan: Methodology. Rui Liu: Funding acquisition, Conceptualization, Project administration, Investigation, Validation. Xuefeng Yang: Conceptualization, Project administration, Resources, Supervision Validation, Methodology, Writing – review and editing.

Funding

This work was supported by the National Natural Science Foundation of China (no. 82003463).

Availability of data and materials

All the data that support the findings of this study are available from the corresponding author upon reasonable request.

Declarations

Ethics approval and consent to participate

All procedures of animals were approved by the Ethics Committee of Tongji Medical College of Huazhong University of Science and Technology (IACUC number: 2946), which complied with animal biomedical research principles formulated by the China Animal Care Committee and the Council of the International Medical Organization.

Competing interests

The authors declare no competing interests.

Received: 8 August 2024 Accepted: 27 November 2024
Published online: 23 December 2024

References

1. Long JM, Holtzman DM. Alzheimer disease: an update on pathobiology and treatment strategies. Cell. 2019;179(2):312–39.
2. De Felice FG, Ferreira ST. Inflammation, defective insulin signaling, and mitochondrial dysfunction as common molecular denominators connecting type 2 diabetes to Alzheimer disease. Diabetes. 2014;63(7):2262–72.
3. Gudala K, Bansal D, Schifano F, Bhansali A. Diabetes mellitus and risk of dementia: a meta-analysis of prospective observational studies. J Diabetes Invest. 2013;4(6):640–50.
4. Selkoe DJ, Hardy J. The amyloid hypothesis of Alzheimer's disease at 25 years. EMBO Mol Med. 2016;8(6):595-608-08.
5. Guo Y, Wang Q, Chen S, Xu C. Functions of amyloid precursor protein in metabolic diseases. Metabolism. 2021;115: 154454.
6. Hardy J, Selkoe DJ. The amyloid hypothesis of Alzheimer's disease: progress and problems on the road to therapeutics. Science. 2002;297(5580):353–6.
7. Vityala Y, Tagaev T, Ramanujam SK, Kalapala IH, Kaggallu AB, Sultana S, et al. The association of insulin resistance and mild cognitive impairment in elderly patients with alzheimer's disease. Metabolism. 2024;153: 155850.
8. Wakabayashi T, Yamaguchi K, Matsui K, Sano T, Kubota T, Hashimoto T, et al. Differential effects of diet- and genetically-induced brain insulin resistance on amyloid pathology in a mouse model of Alzheimer's disease. Mol Neurodegener. 2019;14(1):15.
9. Lu Y, Wang Y, Ong CN, Subramaniam T, Choi HW, Yuan JM, et al. Metabolic signatures and risk of type 2 diabetes in a Chinese population: an untargeted metabolomics study using both LC-MS and GC-MS. Diabetologia. 2016;59(11):2349–59.
10. Bogl LH, Kaye SM, Rämö JT, Kangas AJ, Soininen P, Hakkarainen A, et al. Abdominal obesity and circulating metabolites: a twin study approach. Metabolism. 2016;65(3):111–21.
11. Neinast MD, Jang C, Hui S, Murashige DS, Chu Q, Morscher RJ, et al. Quantitative analysis of the whole-body metabolic fate of branched-chain amino acids. Cell Metab. 2019;29(2):417–29.
12. Shin AC, Fasshauer M, Filatova N, Grundell LA, Zielinski E, Zhou JY, et al. Brain insulin lowers circulating BCAA levels by inducing hepatic BCAA catabolism. Cell Metab. 2014;20(5):898–909.

13. Zhou M, Shao J, Wu C-Y, Shu L, Dong W, Liu Y, et al. Targeting BCAA catabolism to treat obesity-associated insulin resistance. Diabetes. 2019;68(9):1730–46.
14. Sperringer JE, Addington A, Hutson SM. Branched-chain amino acids and brain metabolism. Neurochem Res. 2017;42(6):1697–709.
15. Polis B, Samson AO. Role of the metabolism of branched-chain amino acids in the development of Alzheimer's disease and other metabolic disorders. Neural Regen Res. 2020;15(8):1460–70.
16. Li H, Ye D, Xie W, Hua F, Yang Y, Wu J, et al. Defect of branched-chain amino acid metabolism promotes the development of Alzheimer's disease by targeting the mTOR signaling. Biosci Rep. 2018;38(4): BSR20180127.
17. Siddik MAB, Mullins CA, Kramer A, Shah H, Gannaban RB, Zabet-Moghaddam M, et al. Branched-chain amino acids are linked with alzheimer's disease-related pathology and cognitive deficits. Cells. 2022;11(21):3523.
18. Natunen T, Martiskainen H, Marttinen M, Gabbouj S, Koivisto H, Kemppainen S, et al. Diabetic phenotype in mouse and humans reduces the number of microglia around β-amyloid plaques. Mol Neurodegener. 2020;15(1):66.
19. Henry RJ, Barrett JP, Vaida M, Khan NZ, Makarevich O, Ritzel RM, et al. Interaction of high-fat diet and brain trauma alters adipose tissue macrophages and brain microglia associated with exacerbated cognitive dysfunction. J Neuroinflamm. 2024;21(1):113.
20. Wang X, He Q, Zhou C, Xu Y, Liu D, Fujiwara N, et al. Prolonged hypernutrition impairs TREM2-dependent efferocytosis to license chronic liver inflammation and NASH development. Immunity. 2023;56(1):58–77.
21. Keren-Shaul H, Spinrad A, Weiner A, Matcovitch-Natan O, Dvir-Szternfeld R, Ulland TK, et al. A unique microglia type associated with restricting development of Alzheimer's disease. Cell. 2017;169(7):1276–90.
22. Choi I, Wang M, Yoo S, Xu P, Seegobin SP, Li X, et al. Autophagy enables microglia to engage amyloid plaques and prevents microglial senescence. Nat Cell Biol. 2023;25(7):963–74.
23. Zhao Y, Wu X, Li X, Jiang L-L, Gui X, Liu Y, et al. TREM2 is a receptor for β-amyloid that mediates microglial function. Neuron. 2018;97(5):1023–31.
24. Olufunmilayo EO, Holsinger RMD. Variant TREM2 signaling in Alzheimer's disease. J Mol Biol. 2022;434(7): 167470.
25. Wang S, Sudan R, Peng V, Zhou Y, Du S, Yuede CM, et al. TREM2 drives microglia response to amyloid-β via SYK-dependent and -independent pathways. Cell. 2022;185(22):4153–69.
26. Song WM, Joshita S, Zhou Y, Ulland TK, Gilfillan S, Colonna M. Humanized TREM2 mice reveal microglia-intrinsic and -extrinsic effects of R47H polymorphism. J Exp Med. 2018;215(3):745–60.
27. De Simone R, Vissicchio F, Mingarelli C, De Nuccio C, Visentin S, Ajmone-Cat MA, et al. Branched-chain amino acids influence the immune properties of microglial cells and their responsiveness to pro-inflammatory signals. BBA-Mol Basis Dis. 2013;1832(5):650–9.
28. Shen J, Guo H, Liu S, Jin W, Zhang Z-W, Zhang Y, et al. Aberrant branched-chain amino acid accumulation along the microbiota–gut–brain axis: crucial targets affecting the occurrence and treatment of ischaemic stroke. Brit J Pharmacol. 2023;180(3):347–68.
29. Kober DL, Brett TJ. TREM2-ligand interactions in health and disease. J Mol Biol. 2017;429(11):1607–29.
30. Wood JI, Wong E, Joghee R, Balbaa A, Vitanova KS, Stringer KM, et al. Plaque contact and unimpaired Trem2 is required for the microglial response to amyloid pathology. Cell Rep. 2022;41(8): 111686.
31. Lachance V, Wang Q, Sweet E, Choi I, Cai CZ, Zhuang XX, et al. Autophagy protein NRBF2 has reduced expression in Alzheimer's brains and modulates memory and amyloid-beta homeostasis in mice. Mol Neurodegener. 2019;14(1):43.
32. Cho MH, Cho K, Kang HJ, Jeon EY, Kim HS, Kwon HJ, et al. Autophagy in microglia degrades extracellular β-amyloid fibrils and regulates the NLRP3 inflammasome. Autophagy. 2014;10(10):1761–75.
33. Heckmann BL, Teubner BJW, Tummers B, Boada-Romero E, Harris L, Yang M, et al. LC3-associated endocytosis facilitates β-amyloid clearance and mitigates neurodegeneration in murine Alzheimer's disease. Cell. 2019;178(3):536–51.
34. Bathena SP, Huang J, Epstein AA, Gendelman HE, Boska MD, Alnouti Y. Rapid and reliable quantitation of amino acids and myo-inositol in mouse brain by high performance liquid chromatography and tandem mass spectrometry. J Chromatogr B. 2012;893–894:15–20.
35. Sargsyan M, Trchounian A. Development and validation of LC-MS/MS method for determination of branched chain amino acids and α-keto acids in human plasma. Int J Mass Spectrom. 2020;453: 116345.
36. Pan R-Y, Ma J, Kong X-X, Wang X-F, Li S-S, Qi X-L, et al. Sodium rutin ameliorates Alzheimer's disease–like pathology by enhancing microglial amyloid-β clearance. Sci Adv. 2019;5(2):eaau328.
37. Xue T, Ji J, Sun Y, Huang X, Cai Z, Yang J, et al. Sphingosine-1-phosphate, a novel TREM2 ligand, promotes microglial phagocytosis to protect against ischemic brain injury. Acta Pharm Sin B. 2022;12(4):1885–98.
38. Szykowska A, Chen Y, Smith TB, Preger C, Yang J, Qian D, et al. Selection and structural characterization of anti-TREM2 scFvs that reduce levels of shed ectodomain. Structure. 2021;29(11):1241–52.
39. Almqvist H, Axelsson H, Jafari R, Dan C, Mateus A, Haraldsson M, et al. CETSA screening identifies known and novel thymidylate synthase inhibitors and slow intracellular activation of 5-fluorouracil. Nature Commun. 2016;7(1):11040.
40. Reiserer RS, Harrison FE, Syverud DC, McDonald MP. Impaired spatial learning in the APPSwe + PSEN1ΔE9 bigenic mouse model of Alzheimer's disease. Genes Brain Behav. 2007;6(1):54–65.
41. Macklin L, Griffith CM, Cai Y, Rose GM, Yan X-X, Patrylo PR. Glucose tolerance and insulin sensitivity are impaired in APP/PS1 transgenic mice prior to amyloid plaque pathogenesis and cognitive decline. Exp Gerontol. 2017;88:9–18.
42. Bixel MG, Shimomura Y, Hutson SM, Hamprecht B. Distribution of key enzymes of branched-chain amino acid metabolism in glial and neuronal cells in culture. J Histochem Cytochem. 2001;49(3):407–18.
43. Hull J, Usmari Moraes M, Brookes E, Love S, Conway ME. Distribution of the branched-chain alpha-ketoacid dehydrogenase complex E1alpha subunit and glutamate dehydrogenase in the human brain and their role in neuro-metabolism. Neurochem Int. 2018;112:49–58.
44. Sun Y, Ma C, Sun H, Wang H, Peng W, Zhou Z, et al. Metabolism: a novel shared link between diabetes mellitus and Alzheimer's disease. J Diabetes Res. 2020;2020:4981814.
45. Pang K, Jiang R, Zhang W, Yang Z, Li L-L, Shimozawa M, et al. An App knock-in rat model for Alzheimer's disease exhibiting Aβ and tau pathologies, neuronal death and cognitive impairments. Cell Res. 2022;32(2):157–75.
46. Sheng M, Sabatini BL, Südhof TC. Synapses and Alzheimer's disease. Cold Spring Harbor Perspect Biol. 2012;4: a005777.
47. Jackson J, Jambrina E, Li J, Marston H, Menzies F, Phillips K, et al. Targeting the synapse in Alzheimer's disease. Front Neurosci-Switz. 2019;13:735.
48. Mawuenyega KG, Sigurdson W, Ovod V, Munsell L, Kasten T, Morris JC, et al. Decreased clearance of CNS β-amyloid in Alzheimer's disease. Science. 2010;330(6012):1774–874.
49. Neinast M, Murashige D, Arany Z. Branched chain amino acids. Annu Rev Physiol. 2019;81:139–64.
50. Peña-Martinez C, Rickman AD, Heckmann BL. Beyond autophagy: LC3-associated phagocytosis and endocytosis. Sci Adv. 2022;8(43):eabn1702.
51. Jacquin E, Leclerc-Mercier S, Judon C, Blanchard E, Fraitag S, Florey O. Pharmacological modulators of autophagy activate a parallel noncanonical pathway driving unconventional LC3 lipidation. Autophagy. 2017;13(5):854–67.
52. Shen S, Cheng X, Zhou L, Zhao Y, Wang H, Zhang J, et al. Neutrophil nanovesicle protects against experimental autoimmune encephalomyelitis through enhancing myelin clearance by microglia. ACS Nano. 2022;16(11):18886–97.
53. Jankowsky JL, Xu G, Fromholt D, Gonzales V, Borchelt DR. Environmental enrichment exacerbates amyloid plaque formation in a transgenic mouse model of alzheimer disease. J Neuropath Exp Neur. 2003;62(12):1220–7.
54. Yang T, Zhang S, Yuan H, Wang Y, Cai L, Chen H, et al. Platinum-based TREM2 inhibitor suppresses tumors by remodeling the immunosuppressive microenvironment. Angew Chem. 2023;62(2): e202213337.
55. Kober DL, Stuchell-Brereton MD, Kluender CE, Dean HB, Strickland MR, Steinberg DF, et al. Functional insights from biophysical study of TREM2 interactions with apoE and Aβ1-42. Alzheimers Dement. 2021;17(3):475–88.
56. Jafari R, Almqvist H, Axelsson H, Ignatushchenko M, Lundbäck T, Nordlund P, et al. The cellular thermal shift assay for evaluating drug target interactions in cells. Nat Protoc. 2014;9(9):2100–22.

57. Florey O, Gammoh N, Kim SE, Jiang X, Overholtzer M. V-ATPase and osmotic imbalances activate endolysosomal LC3 lipidation. Autophagy. 2015;11(1):88–99.
58. Luo ZL, Sheng ZY, Hu LY, Shi L, Tian YC, Zhao XC, et al. Targeted macrophage phagocytosis by Irg1/itaconate axis improves the prognosis of intracerebral hemorrhagic stroke and peritonitis. EBioMedicine. 2024. https://doi.org/10.1016/j.ebiom.2024.104993.

Publisher's Note